Clinical Biomechanics 25 (2010) 372–377

Contents lists available at ScienceDirect

Clinical Biomechanics

journal homepage: www.elsevier.com/locate/clinbiomech

Effects of running speed on a probabilistic stress fracture model

W. Brent Edwards [a,b,*], David Taylor [c], Thomas J. Rudolphi [d], Jason C. Gillette [b], Timothy R. Derrick [b]

[a] Department of Kinesiology and Nutrition, University of Illinois at Chicago, Chicago, IL 60612, USA
[b] Department of Kinesiology, Iowa State University, Ames, IA 50011, USA
[c] Trinity Centre for Bioengineering, Department of Mechanical and Manufacturing Engineering, Trinity College Dublin, Dublin 2, Ireland
[d] Department of Aerospace Engineering, Iowa State University, Ames, IA 50011, USA

ARTICLE INFO

Article history:
Received 15 October 2009
Accepted 5 January 2010

Keywords:
Bone fatigue
Overuse injury
Tibia
Musculoskeletal model

ABSTRACT

Background: Stress fractures are dependent on both loading magnitude and loading exposure. Decreasing speed is a potential mechanism of strain reduction during running. However, if running speed is decreased the number of loading cycles will increase for a given mileage. It is unclear if these increased loading cycles are detrimental despite reductions in bone strain. The purpose of this study was to determine the effects of running speed on the probability of tibial stress fracture during a new running regimen.

Methods: Ten male subjects ran overground at 2.5, 3.5, and 4.5 m/s. Force platform and kinematic data were collected synchronously. Inverse dynamics and musculoskeletal modeling were used to determine joint contact forces acting on the distal tibia. Peak tibial contact force served as input to a finite element model to estimate tibial strains. Stress fracture probability for each running speed was determined using a probabilistic model based on published relationships of bone damage, repair, and adaptation. The effects of speed on stress fracture probability was compared using a repeated measures ANOVA.

Findings: Decreasing running speed from 4.5 to 3.5 m/s reduced the estimated likelihood for stress fracture by 7% ($P = 0.017$). Decreasing running speed from 3.5 to 2.5 m/s further reduced the likelihood for stress fracture by 10% ($P < 0.001$).

Interpretation: Runners wanting to reduce their risk for tibial stress fracture may benefit from a decrease in running speed. For the speeds and mileage relative to the current study, stress fracture development was more dependent on loading magnitude rather than loading exposure.

1. Introduction

Running is a leisure activity of choice for many. Unfortunately, it is estimated that 26–65% of runners, both recreational and competitive, will sustain some form of overuse injury during any given year (Caspersen et al., 1984; Lysholm and Wiklander, 1987; Marti et al., 1988). Stress fractures may account for approximately 15–20% of overuse injuries (Bennell et al., 1996a; Brubaker and James, 1974). Although stress fractures can materialize within any load-bearing bone, they frequently develop in the tibia (Korpelainen et al., 2001; Milgrom et al., 1985).

Stress fractures result, in part, from the mechanical fatigue of bone (Burr et al., 1990). Over time, cyclical loading results in material property degradation (Pattin et al., 1996) as microcracks are nucleated within the bony matrix (Burr et al., 1998). If the energy release rate, or "crack driving force", is greater than the microstructure's crack resistance, microcracks will propagate into macrocracks, or stress fractures. The crack driving force increases with loading magnitude and crack length (Martin et al., 1998). When loading magnitude is low, it is believed that bone will have sufficient time for remodeling; the microcrack will be completely removed or reduced in size, and a stress fracture will not occur. Conversely, high magnitude loading increases the rate of microcrack nucleation and subsequently overwhelms the repair process (Frost, 1998). Identifying loading patterns that reduce bone strain may therefore aid in the prevention of stress fracture.

The fatigue life of bone, as a function of applied load, can be described using an inverse power-law relationship (Carter and Caler, 1985). Indeed, small changes in load result in large changes in the number of cycles to failure. However, it is also true that many cycles of low magnitude loading may be as, or more, detrimental than fewer cycles of high magnitude loading. Reducing running speed is a potential mechanism of load reduction during running. A positive relationship between ground reaction force and speed has been well established (Keller et al., 1996; Munro et al., 1987). Intuition suggests that a similar relationship exists for bone strain. Furthermore, a reduction in running speed also requires an

* Corresponding author. Address: Department of Kinesiology and Nutrition, University of Illinois at Chicago, 1919 W. Taylor Street, 650 AHSB, M/C 517, Chicago, IL 60612, USA.
E-mail address: edwardsb@uic.edu (W.B. Edwards).

0268-0033/$ - see front matter © 2010 Elsevier Ltd. All rights reserved.
doi:10.1016/j.clinbiomech.2010.01.001

increased number of loading cycles for a given mileage (assuming a positive relationship between running speed and stride length). Consequently, it is unclear if the benefits of decreased strain with running speed reduction outweigh the detriments of increased loading cycles required for a given running mileage.

The purpose of this study was to determine the influence of running speed on the probability of tibial stress fracture during a new running regimen. We hypothesized that reducing running speed would decrease tibial strain enough to negate the detrimental increased number of loading cycles associated with the reduction. This would lead to a reduction in the probability of tibial stress fracture with a corresponding decrease in running speed. To answer this question we simulated the first 100 days of training using a probabilistic model of bone damage, repair, and adaptation.

2. Methods

2.1. Subjects

A convenience sample of 10 males were recruited for this study (age 24.9 (SD 4.7) years; height 1.7 (SD 0.1) m; mass 70.1 (SD 8.9) kg). All subjects participated in running, or athletic activity requiring running, on a weekly basis. Inclusion criteria required subjects to be free from lower-extremity injuries resulting in the disruption of normal physical activity for atleast 3 months before study participation. Prior to data collection, the experimental protocol was approved by the institutional review board and subjects provided written informed consent.

2.2. Experimental data collection

Subjects arrived at the lab wearing their personal running shoes and were outfitted with tight fitting athletic clothing. A single researcher took anthropometric measurements and placed retroreflective markers overlying the skin of anatomical landmarks of the trunk and right lower-extremity. Markers were adhered to the dorsi-foot, fifth metatarsal, heel, medial and lateral malleolus, distal and proximal anterior calf, posterior calf, medial and lateral femoral epicondyle, anterior and lateral thigh, left and right greater trochanter, left and right anterior superior iliac spine, and the joint between the fifth lumbar and first sacrum (L5S1). A static motion capture trial was collected while the subject stood in the anatomical position to establish joint center locations. Joint centers were assumed to be stationary in the segmental coordinate systems. Segmental coordinate systems were defined using a right handed rule. The x-axes were oriented in the anterior–posterior (AP) direction, the y-axes were oriented in the axial direction, and the z-axes were oriented in the medial–lateral (ML) direction. The subtalar joint axis was determined in accordance with O'Connor and Hamill (2005). The x-axis of the foot was transformed to the subtalar axis by rotating the foot coordinate system 44° upward about the z-axis, and 17° medial about the y-axis. This transformation was based on the average subtalar axis orientation reported by Inman (1976).

Subjects were instructed to run overground at three prescribed speeds (2.5, 3.5, and 4.5 m/s); speed order was randomized across subjects. Motion capture (Vicon MX, Vicon, Centennial, CO, USA) and force platform (AMTI, Watertown, MA, USA) data were collected synchronously at sampling frequencies of 160 and 1600 Hz, respectively. Running speed was monitored via motion capture using the horizontal component of the L5S1 marker. The length of the laboratory runway was 28.5 m, but was only used in its entirety during faster running conditions. Ten trials were performed at each speed. Trials were accepted if the speed was within 5% of the prescribed speed and the subject's right foot hit the force platform with no visually identifiable targeting. During each trial a researcher used a stop watch to measure the time it took for the subject to take three strides. These data were used to determine the subjects' average stride frequency and stride length at each speed.

2.3. Data processing

The raw motion capture and force platform data were exported to Matlab (The Mathworks, Natick, MA, USA) for data processing. Using a 4th order zero-lag Butterworth filter, motion capture and force platform data were smoothed at identical cutoff frequencies (van den Bogert and de Koning, 1996). For an objective measure, the cutoff frequency corresponded to the 95th percentile frequency of the vertical ground reaction force. The 95th percentile frequency was calculated from the cumulative sum of an integrated power spectral density curve. The resulting mean cutoff frequencies were 20.3 (SD 3.1), 26.6 (SD 2.8), and 32.8 (SD 3.9) Hz, for the 2.5, 3.5, and 4.5 m/s conditions, respectively. Three-dimensional Cardan joint and segment angles were determined using a flexion–extension, abduction–adduction, internal–external rotation sequence. Joint reaction forces and net internal joint moments were determined using standard inverse dynamics with rigid body assumptions. Segment masses, moments of inertia, and center of mass locations were calculated using the anthropometrics measured prior to data collection (Vaughan et al., 1992). The subtalar joint moment was estimated by transforming the ankle joint moment into the subtalar coordinate system.

2.4. Musculoskeletal modeling

The stance phase joint angles were interpolated to 101 points using a cubic-spine technique and imported to a SIMM musculoskeletal model (Musculo-Graphics Inc., Santa Rosa, CA, USA) that was scaled to each individual's segment lengths. The SIMM model (Delp et al., 1990) consisted of 43 lower-extremity muscles and was used to estimate maximum dynamic muscle forces (adjusted for muscle length and velocity), muscle moment arms, and muscle orientations in the segmental coordinate systems (Delp and Loan, 1995).

Individual muscle forces were estimated with static optimization using a cost function to minimize the sum of squared muscle stresses (Glitsch and Baumann, 1997). The optimization was constrained such that when the muscle forces were multiplied by their respective moment arms the solution equaled the experimentally determined joint moments. Six moments were utilized as constraints including the three orthogonal components at the hip, the flexion–extension moment at the knee and ankle, and the subtalar moment. Lower and upper bound muscle forces were initially set to zero and the maximum dynamic muscle forces, respectively. These bounds were adjusted in subsequent frames to prevent non-physiological changes in muscle force (Pierrynowski and Morrison, 1985). This optimization routine, apart from the utilization of the subtalar moment, has been previously described (Edwards et al., 2008).

The ankle joint contact force was calculated as the vector sum of the reaction force and muscle forces crossing the talocrural joint. It was assumed that 10% of the ankle joint contact force was borne by the fibula (Sasimontonkul et al., 2007). Thus, the contact force acting on the tibia was calculated as:

$$Fc^t = 0.9 \cdot \left[RF^a + \sum_{i=31}^{43} f_i \right] \quad (1)$$

where Fc^t is the three components of the joint contact force acting on the tibia, RF^a is the three components of the joint reaction force

acting on the ankle, and f_i is the three components of the ith predicted muscle force crossing the ankle joint (muscles $i = 1$–30 do not cross the ankle).

Maximum tibial strains for each speed were determined using the finite element method. The tibia was modeled with 5,391 8-node hexahedral elements (total degrees of freedom: 6340) based on publically available data (VAKHUM data set; URL: http://www.ulb.ac.be/project/vakhum/); the fibula was not considered. The peak instantaneous contact force, averaged across trials, was applied as a distributed load to the distal end of the tibia and the proximal end was fully constrained. A separate model was created for each subject that was scaled longitudinally to leg length, and radially assuming bone mass scales to body mass, or length·diameter$^2 \propto$ body mass (McMahon, 1973). Material properties were assumed to be linear elastic and isotropic, with cortical bone having a Young's modulus of 18.6 GPa, and trabecular bone a Young's modulus of 10.4 GPa (Rho et al., 1993). Poisson's ratio for both materials was 0.3. All models were solved using FEBio software (Musculoskeletal Research Laboratories, Salt Lake City, UT, USA; URL: http://www.mrl.sci.utah.edu/software.php?soft_id=7). A total of 30 finite element simulations were performed (3 speeds $\times$ 10 subjects).

2.5. Probabilistic model of stress fracture

The likelihood for tibial stress fracture was determined using a probabilistic model of bone damage, repair, and adaptation. A brief overview of the model and its equations are introduced below; equation constants for the application presented herein have been previously reported (Edwards et al., 2009). For a comprehensive review, theoretical development, and sample demonstrations of the model the reader is referred to Taylor (1998), Taylor and Kuiper (2001), and Taylor et al. (2004).

The fatigue life of a bone can be described using the standard fatigue equation:

$$N_f = C\Delta\varepsilon^{-n}. \tag{2}$$

Therefore, if we know the strain range $\Delta\varepsilon$, and experimentally derived constants n and C, we can determine the number of loading cycles to failure N_f. For *in vivo* applications $\Delta\varepsilon$ equals maximum strain magnitude because minimum strain magnitude during a stride cycle is close to zero.

The maximum absolute principal strains were obtained for each element. However, because we are simulating the first 100 days of a new training regimen, bone adaptation will take place in response to mechanical loading. This will result in an increase in cross sectional area and areal moment of inertia of the bone such that tibial strains are reduced over time. Assuming a maximum rate of lamellar bone deposition of 4 μm/day (Turner et al., 1994) on the periosteal surface, we obtained an adaptation "strain ratio" using equations of beam theory. The strain ratio was defined as the ratio of strain after bone deposition to strain with original bone geometry. This ratio was multiplied by the $\Delta\varepsilon$ to determine changes in tibial strain over time due to bone adaptation. An equivalent strain for each element that accounted for adaptation was then determined (Taylor et al., 2004):

$$\Delta\varepsilon_{eq} = \left(\frac{1}{t_T}\int_0^{t_T}\Delta\varepsilon^n dt\right)^{1/n} \tag{3}$$

where t_T is the total time over which adaptation takes place (i.e., 100 days).

The $\Delta\varepsilon_{eq}$, accounting for adaptation, can be used within the standard fatigue equation to obtain N_f. However, due to inherent microstructural differences in experimental testing specimens, considerable scatter in the fatigue life of bone is present. A common procedure in fatigue mechanics used to determine the probability of failure when there is considerable scatter in a materials fatigue behavior is the Weibull approach. The model used a modified Weibull equation that accounted for stressed volume (Taylor et al., 2004):

$$P_{fa} = 1 - \exp\left[-\left(\frac{V_s}{V_{so}}\right)\left(\frac{t}{t_f}\right)^w\right] \tag{4}$$

where V_{so} is the reference stressed volume, t_f is the reference time until failure at the applied strain range and number of loading cycles/day, and w expresses the degree of scatter in the material. These constants were derived from experimental fatigue testing literature and allowed us to predict the cumulative probability of failure with adaptation P_{fa} for a specimen having stressed volume V_s from time zero to t. Accounting for stressed volume is important when considering whole bone fatigue because small experimental testing specimens are inherently stronger than large specimens (i.e., small specimens have fewer "weak" points) (Taylor, 1998).

As $\Delta\varepsilon_{eq}$ varies across the entire bone, P_{fa} is not constant throughout the tibia. Using the finite element method we obtained a separate P_{fa} for each element. Given a model consisting of k elements, then P_{fa} for the entire tibia was the probability that any one element would fail, thus (Taylor and Kuiper, 2001):

$$P_{fa} = 1 - (1 - P_1)(1 - P_2)(1 - P_3)\ldots(1 - P_k). \tag{5}$$

For convenience, elements experiencing similar strains were grouped together; for the tibia, Taylor and Kuiper (2001) found that eight groups could be used without significant error. The corresponding V_s for each group were obtained by summing individual element volumes within the eight groups. Using the strain values from the mid-points of each group and the corresponding V_s (multiplied by 2 to account for both legs) we used Eq. (5) to determine a single P_{fa} for both tibias.

There is considerable variability in the time it takes for a basic multicellular unit to sufficiently tunnel through and repair a microcrack. Taylor et al. (2004) estimated this time to be 18.5 days with an associated standard deviation of 12.5 days. Thus, we described the cumulative probability of bone repair P_r with a second Weibull equation (Taylor et al., 2004):

$$P_r = 1 - \exp\left[-\left(\frac{t}{t_r}\right)^v\right] \tag{6}$$

where t_r is the reference time for repair and v expresses the degree of scatter in repair time. By determining the probability that bone will not repair itself $(1 - P_r)$ and multiplying it by the instantaneous probability that failure with adaptation will take place (time differential of P_{fa}), we obtained an instantaneous probability that accounted for failure, repair and adaptation; integrating with respect to time gave the cumulative probability of failure with repair and adaptation (P_{fra}). For each running condition we assumed subjects ran 4.8 km/day (3.0 miles/day). Loading cycles/day were estimated by dividing running mileage by average stride length.

2.6. Statistics

Peak P_{fra} over the course of 100 days was determined for each subject and running speed. Differences in peak P_{fra}, as a function of running speed, were compared using a one-way repeated measures ANOVA. Statistical analyses were performed in SPSS (SPSS, Inc., Chicago, IL, USA) with the criterion alpha level set to 0.05. In the event of a significant main effect of running speed we used Bonferroni adjusted post hoc comparisons (alpha = 0.05/3 = 0.017).

3. Results

In general, the joint contact force acting on the distal tibia increased with running speed (Fig. 1). The axial component, directed along the longitudinal axis of the tibia, was the dominant force. The AP component was only slightly larger than the ML component. The mean peak instantaneous tibial contact forces used as inputs to the finite element models are displayed in Table 1. At the instant of peak instantaneous resultant force the shear components were directed posteriorly and laterally.

The tibia was loaded in bending and axial compression. This type of combined loading resulted in compressive principal strain on the posterior surface that was larger than the tensile principal strain on the anterior surface (Fig. 2). Peak principal strains increased with running speed with mean peak strains ranging from 3595 to 4577 με (Table 2).

Due to the positive relationship between locomotion speed and stride length, the number of loading exposures decreased with running speed (Table 2). Assuming a daily running regimen of 4.8 km/day, the number of loading exposures were 2435, 1829, and 1549 cycles/day for 2.5, 3.5, and 4.5 m/s, respectively.

The probability of failure P_{fra} peaked and leveled off after approximately 40 days of training (Fig. 3). A reduction in running speed resulted in a corresponding reduction in P_{fra}. Specifically, decreasing running speed from 4.5 to 3.5 m/s reduced mean P_{fra} by 7% ($P = 0.017$), while decreasing running speed from 3.5 to 2.5 m/s reduced mean P_{fra} by 10% ($P < 0.001$; Table 2). The within subject response was consistent across running conditions with the exception of one case for subject 10 (Fig. 4). For subject 10, changing running speed from 4.5 to 3.5 m/s resulted in a small increase in P_{fra} of 0.9%.

4. Discussion

The purpose of this study was to determine if decreasing running speed reduced the probability of tibial stress fracture during a new running regimen. Our hypothesis that reducing running speed would decrease tibial strain sufficiently enough to negate the detrimental increase in loading cycles associated with a given running mileage was supported by the results of this study. Specifically, a reduction in running speed resulted in a corresponding reduction in the probability of tibial stress fracture.

Stress fractures tend to materialize during the first 2–8 weeks of a new training regimen (Burr, 1997). This time frame is consistent with our cumulative probability of failure P_{fra} peaking and leveling off after approximately 5.7 weeks or 40 days of training. Our mean peak probabilities of failure ranged from 9% to 26%. These values are only slightly higher than the 10–20% annual incidence rate of stress fracture in male track and field athletes (Bennell et al., 1996b; Johnson et al., 1994).

Table 1
Mean (SD) tibial contact force across running speeds used as inputs to the finite element models. Values represent the instant of peak resultant force. Positive numbers indicate anterior shear, axial compression, and lateral shear.

Speed (m/s)	Tibial contact force (BW)		
	Anterior–posterior	Axial	Medial–lateral
2.5	−0.53 (0.06)	10.73 (1.03)	0.51 (0.18)
3.5	−0.62 (0.07)	12.63 (1.19)	0.61 (0.21)
4.5	−0.66 (0.09)	13.80 (1.63)	0.68 (0.22)

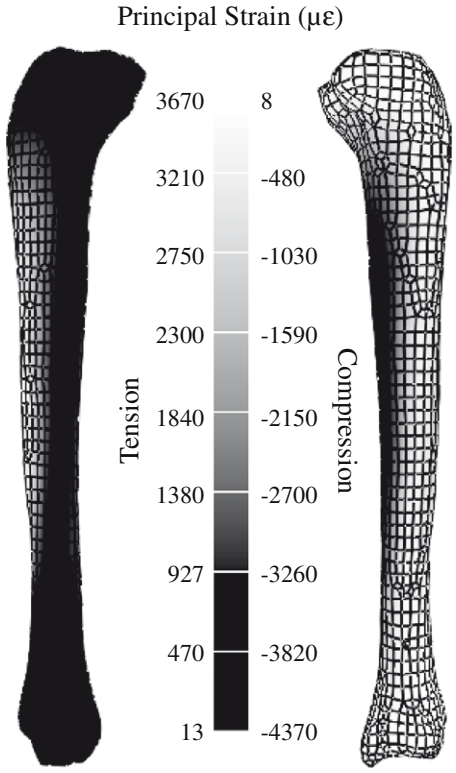

Fig. 2. Sagittal views of a representative finite element model of the tibia displaying maximum principal strains during running. The models were loaded in bending and axial compression with peak compression on the posterior surface (right) and peak tension on the anterior surface (left).

We previously reported a 10% mean probability of tibial stress fracture for subjects running 4.8 km/day at 4.4 m/s (Edwards et al., 2009). This value is considerably lower than the 26% reported here for subjects running at 4.5 m/s. Two explanations can be given for this discrepancy: first, our previous study did not include the

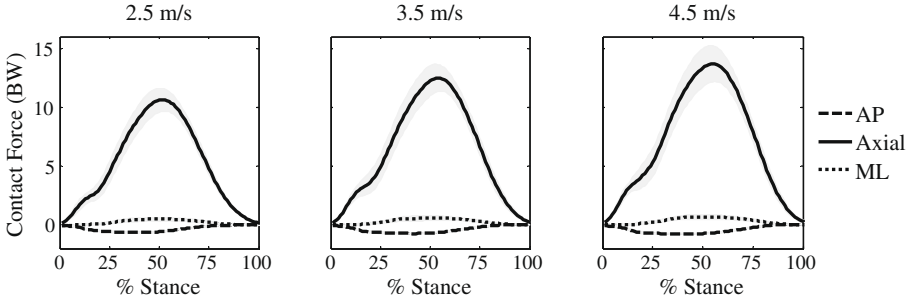

Fig. 1. Ensemble average tibial contact forces across running speeds. Positive numbers indicate anterior shear, axial compression, and lateral shear.

Table 2
Mean (SD) absolute peak principal strain, daily loading exposure, and probability of failure P_{fra} across running speeds.

	Speed (m/s)		
	2.5	3.5	4.5
Peak principal strain (με)	3594.94 (434.63)	4239.39 (474.25)	4576.85 (547.96)
Loading exposure (cycles/day)	2434.83 (93.89)	1829.30 (74.16)	1549.26 (72.65)
Probability of failure (P_{fra})	0.09 (0.12)*	0.19 (0.13)*	0.26 (0.15)*

* Significantly different from all other running speeds ($P < 0.017$).

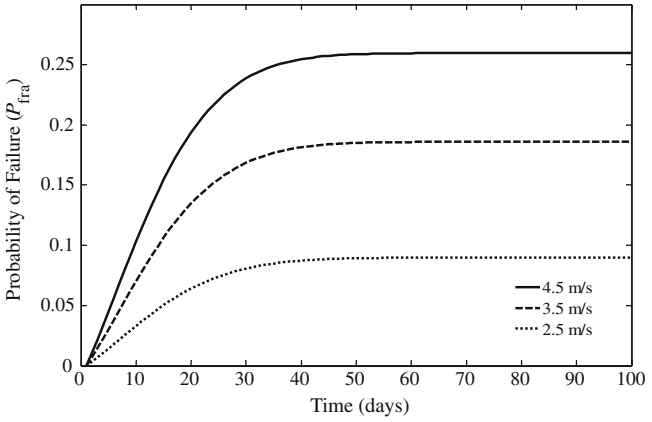

Fig. 3. Ensemble average probabilities of failure (P_{fra}) for 100 days of training.

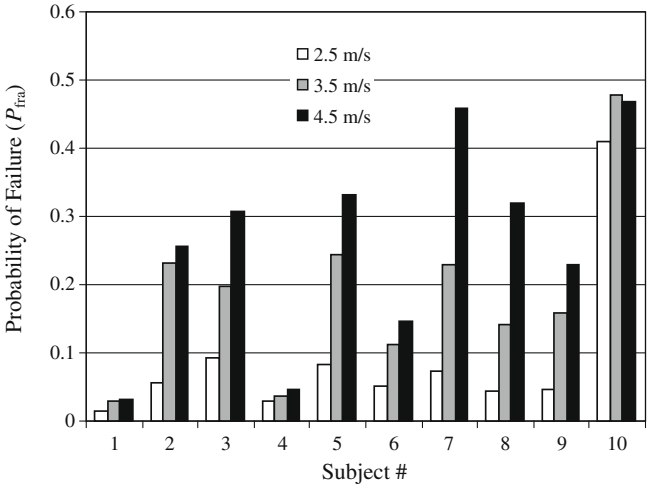

Fig. 4. Within subject response for peak probabilities of failure (P_{fra}).

subtalar moment within the muscle optimization. As a result, the axial tibial contact force was slightly higher in this study (present mean value of 13.8 BW compared to a previous mean value of 13.4 BW). Second, we previously excluded the medial–lateral component of the tibial contact force as a finite element boundary condition. This extra shear component aligned the resultant contact force further away from the longitudinal axis of the tibia, creating a larger bending moment. These two refinements to the model substantially increased the mean peak strain (present mean value of 4577 με compared to a previous mean value of 3794 με).

In contrast to the other nine subjects, subject 10's probability of tibial stress fracture increased when running speed was reduced from 4.5 to 3.5 m/s. This subject displayed a corresponding decrease in joint contact force (and tibial strain) with reduced speed, but his relative change in loading magnitude was lowest for the group. Specifically, subject 10's tibial strain decrease by 2%; the mean reduction in tibial strain for the rest of the group was 8(4)%. Additionally, subject 10 did not display a marked difference in loading cycles/day compared to the group mean. This response is directly in line with the impetus for this study, suggesting that a reduction in loading magnitude is not always synonymous with a reduction in stress fracture probability. Rather, there exists a required reduction in strain magnitude necessary to mitigate the increase in loading cycles that result from a reduced speed of running. In the future, perhaps biomechanical analyses can be used on a subject-specific basis to identify those runners who would benefit from alterations in running speed. However, for the speeds and mileage relevant to the current study, our statistical results suggest that a speed decrease of 1 m/s is sufficient to reach the required reduction in strain magnitude for the majority of runners. It is unclear if similar conclusions would be obtained at speeds outside our tested range (2.5–4.5 m/s).

Changes in stride length naturally occur with changes in running speed. There is evidence to suggest that the observed positive relationship between external ground reaction force and running speed is more related to resulting changes in stride length rather than changes in speed itself (Mercer et al., 2005). If this relationship were to hold true for joint contact forces, and runners reduced their speed while maintaining a fixed stride length, reductions in running speed would not be associated with corresponding reductions in tibial strain. The number of loading cycles for a given mileage would not change, and consequently, the probability of tibial stress fracture would stay the same. For this reason, future research should focus on which factor, running speed or stride length, is the critical determinant for joint contact force magnitude.

This study is limited by our inability to account for certain subject specific parameters in our modeling procedures. Even though the musculoskeletal model was scaled to the individual's segment lengths, an underestimation in muscle moment arms can lead to an overestimation in muscle forces when using static optimization. *In vivo* Achilles tendon forces across a range of running speeds have been directly measured with the use a "buckle"-type transducer (Komi, 1990). A least-squares fit of these data would predict peak Achilles tendon forces of 7.5–9.5 BW between running speeds of 3.5 and 4.5 m/s. Adding a reaction force of 2.5 BW one can obtain a conservative ankle joint contact force estimate between 10 and 12 BW. These values are slightly less than the tibial contact forces reported for this study. These differences can be easily explained by the inclusion of the non-triceps surae muscles within our model, and thus, we feel our measure of tibial contact force to be valid.

Our values in stress fracture probability are heavily dependent on the accuracy of tibial strains obtained from our modeling procedures. Our mean peak tibial strains during running ranged from 3595 to 4577 με, which is twice as large as those previously measured *in vivo* (Milgrom et al., 2000). However, it should be emphasized that experimentally determined bone strains from strain gage rosettes are only indicative of the local mechanical environment underneath the gage mounting-location. Clearly, the strain distribution of the tibia during exercise is not uniform throughout due to its complex shape and nature of loading. We did indeed get strains ranging between 1000 and 2000 με at the medial aspect of the mid tibial diaphysis where most experimentally measured strains have been obtained. In addition, strains of 4200 με have been measured on the posteromedial surface of the tibia during

forward jumping (Ekenman et al., 1998), the near location at which we found peak values for our modeling results.

Our models were based on a generic tibia scaled to each subject's body size, and therefore did not account for subject-specific adaptations in geometry and material properties. We tested the sensitivity of our allometric scaling procedure and material property assumptions. Although manipulating these parameters changed the peak strains and probabilities of failure, the statistical relationships and interpretation of the results were maintained. Assuming that our modeling procedure resulted in random variation from actual stress fracture probability, merit should be given to the mean values and relative differences reported in this study.

The probabilistic model of bone damage, repair, and adaptation is designed for individuals beginning a weekly running regimen. For the speeds and mileage relative to the current study, stress fracture development was more dependent on loading magnitude rather than loading exposure. Thus, our results suggest that reducing running speed is an effective kinematic adjustment that can be implemented during the regimen's initial stages to reduce the probability for tibial stress fracture. Once the bone has adapted to the novel mechanical loads placed upon it over the course of the first few months, runners could gradually increase their speed.

References

Bennell, K.L., Malcolm, S.A., Thomas, S.A., Reid, S.J., Brukner, P.D., Ebeling, P.R., et al., 1996a. Risk factors for stress fractures in track and field athletes. A twelve-month prospective study. American Journal of Sports Medicine 24, 810–818.

Bennell, K.L., Malcolm, S.A., Thomas, S.A., Wark, J.D., Brukner, P.D., 1996b. The incidence and distribution of stress fractures in competitive track and field athletes. A twelve-month prospective study. The American Journal of Sports Medicine 24, 211–217.

Brubaker, C.E., James, S.L., 1974. Injuries to runners. Journal of Sports Medicine 2, 189–198.

Burr, D.B., 1997. Bone, exercise, and stress fractures. Exercise and Sport Sciences Reviews 25, 171–194.

Burr, D.B., Milgrom, C., Boyd, R.D., Higgins, W.L., Robin, G., Radin, E.L., 1990. Experimental stress fracture of the tibia. The Journal of Bone and Joint Surgery, 370–375.

Burr, D.B., Turner, C.H., Naick, P., Forwood, M.R., Ambrosius, W., Hasan, M.S., et al., 1998. Does microdamage accumulation affect the mechanical properties of bone? Journal of Biomechanics 31, 337–345.

Carter, D.R., Caler, W.E., 1985. A cumulative damage model for bone fracture. Journal of Orthopaedic Research 3, 84–90.

Caspersen, C.J., Powell, K.E., Koplan, J.P., Shirley, R.W., Campbell, C.C., Sikes, R.K., 1984. The incidence of injuries and hazards in recreational and fitness runners. Medicine and Science in Sport and Exercise 16, 113–114.

Delp, S.L., Loan, J.P., 1995. A graphics-based software system to develop and analyze models of musculoskeletal structures. Computers in Biology and Medicine 25, 21–34.

Delp, S.L., Loan, J.P., Hoy, M.G., Zajac, F.E., Topp, E.L., Rosen, J.M., 1990. An interactive graphics-based model of the lower extremity to study orthopaedic surgical procedures. IEEE Transactions on Biomedical Engineering 37, 757–767.

Edwards, W.B., Gillette, J.C., Thomas, J.M., Derrick, T.R., 2008. Internal femoral forces and moments during running: implications for stress fracture development. Clinical Biomechanics 23, 1269–1278.

Edwards, W.B., Taylor, D., Rudolphi, T.J., Gillette, J.C., Derrick, T.R., 2009. Effects of stride length and running mileage on a probabilistic stress fracture model. Medicine & Science in Sports & Exercise 41, 2177–2184.

Ekenman, I., Halvorsen, K., Westblad, P., Fellander-Tsai, L., Rolf, C., 1998. Local bone deformation at two predominant sites for stress fractures of the tibia: an in vivo study. Foot and Ankle International 19, 479–484.

Frost, H.M., 1998. A brief re view for orthopedic surgeons: fatigue damage (microdamage) in bone (its determinants and clinical implications). Journal of Orthopaedic Science 3, 272–281.

Glitsch, U., Baumann, W., 1997. The three-dimensional determination of internal loads in the lower extremity. Journal of Biomechanics 30, 1123–1131.

Inman, V.T., 1976. The Joints of the Ankle. Williams & Wilkins, Baltimore.

Johnson, A.W., Weiss, C.B., Wheeler, D.L., 1994. Stress fractures of the femoral shaft in athletes-more common than expected: a new clinical test. The American Journal of Sports Medicine 2, 248–256.

Keller, T.S., Weisberger, A.M., Ray, J.L., Hasan, S.S., Shiavi, R.G., Spengler, D.M., 1996. Relationship between vertical ground reaction force and speed during walking, slow jogging, and running. Clinical Biomechanics 11, 253–259.

Komi, P.V., 1990. Relevance of in vivo force measurements to human biomechanics. Journal of Biomechanics 23 (Suppl. 1), 23–34.

Korpelainen, R., Orava, S., Karpakka, J., Siira, P., Hulkko, A., 2001. Risk factors for recurrent stress fracture in athletes. American Journal of Sports Medicine 29, 304–310.

Lysholm, J., Wiklander, J., 1987. Injuries in runners. American Journal of Sports Medicine 15, 168–171.

Marti, B., Vader, J.P., Minder, C.E., Abelin, T., 1988. On the epidemiology of running injuries. The 1984 Bern grand-prix study. American Journal of Sports Medicine 16, 285–294.

Martin, R.B., Burr, D.B., Sharkey, N.A., 1998. Skeletal Tissue Mechanics. Springer-Verlag, New York, USA.

McMahon, T., 1973. Size and shape in biology. Science 179, 1201–1204.

Mercer, J.A., Bezodis, N.E., Russell, M., Purdy, A., DeLion, D., 2005. Kinetic consequences of constraining running behavior. Journal of Sports Science and Medicine 4, 144–152.

Milgrom, C., Finestone, A., Levi, Y., Simkin, A., Ekenman, I., Mendelson, S., et al., 2000. Do high impact exercises produce higher tibial strains than running? British Journal of Sports Medicine 34, 195–199.

Milgrom, C., Giladi, M., Stein, M., Kashtan, H., Margulies, J.Y., Chisin, R., et al., 1985. Stress fractures in military recruits. The Journal of Bone and Joint Surgery, 732–735.

Munro, C.F., Miller, D.I., Fuglevand, A.J., 1987. Ground reaction forces in running: a reexamination. Journal of Biomechanics 20, 147–155.

O'Connor, K.M., Hamill, J., 2005. Frontal plane moments do not accurately reflect ankle dynamics during running. Journal of Applied Biomechanics 21, 85–95.

Pattin, C.A., Caler, W.E., Carter, D.R., 1996. Cyclic mechanical property degradation during fatigue loading of cortical bone. Journal of Biomechanics 29, 69–79.

Pierrynowski, M.R., Morrison, J.B., 1985. A physiological model for the evaluation of muscle forces in human locomotion: theoretical aspects. Mathematical Biosciences 75, 69–101.

Rho, J.Y., Ashman, R.B., Turner, C.H., 1993. Young's modulus of trabecular and cortical bone material: ultrasonic and microtensile measurements. Journal of Biomechanics 26, 111–119.

Sasimontonkul, S., Bay, B.K., Pavol, M.J., 2007. Bone contact forces on the distal tibia during the stance phase of running. Journal of Biomechanics 40, 3503–3509.

Taylor, D., 1998. Fatigue of bone and bones: an analysis based on stressed volume. Journal of Orthopaedic Research 16, 163–169.

Taylor, D., Casolari, E., Bignardi, C., 2004. Predicting stress fractures using a probabilistic model of damage, repair and adaptation. Journal of Orthopaedic Research 22, 487–494.

Taylor, D., Kuiper, J.H., 2001. The prediction of stress fractures using a 'stressed volume' concept. Journal of Orthopaedic Research 19, 919–926.

Turner, C.H., Forwood, M.R., Rho, J.Y., Yoshikawa, T., 1994. Mechanical loading thresholds for lamellar and woven bone formation. Journal of Bone and Mineral Research 9, 87–97.

van den Bogert, A.J., de Koning, J.J., 1996. On optimal filtering for inverse dynamics analysis. In: Paper Presented at the IXth Biennial Conference of the Canadian Society for Biomechanics, Vancouver, BC, Canada.

Vaughan, C.L., Davis, B.L., O'Connor, J.C., 1992. Dynamics of Human Gait. Human Kinetics, Champaign, IL. pp. 84–85.